ORIGINAL ARTICLE

Transcriptional analysis of the intestinal mucosa of patients with ulcerative colitis in remission reveals lasting epithelial cell alterations

Núria Planell,[1,2] Juan J Lozano,[2] Rut Mora-Buch,[1] M Carme Masamunt,[1] Mireya Jimeno,[3] Ingrid Ordás,[1] Miriam Esteller,[1] Elena Ricart,[1] Josep M Piqué,[1] Julián Panés,[1] Azucena Salas[1]

▶ Additional data are published online only. To view these files please visit the journal online (http://dx.doi.org/10.1136/gutjnl-2012-303333).

[1]Department of Gastroenterology, IDIBAPS, Hospital Clínic, CIBER-EHD, Barcelona, Spain
[2]Department of Bioinformatics Platform, CIBERehd, Barcelona, Spain
[3]Department of Pathology, Hospital Clínic, Barcelona, Spain

Correspondence to
Dr Azucena Salas,
Center Esther Koplowitz,
Rosselló 149-153, 3rd Floor,
Barcelona 08036, Spain;
asalas1@clinic.ub.es

Revised 29 August 2012
Accepted 15 September 2012
Published Online First
7 November 2012

ABSTRACT

Objective Ulcerative colitis (UC) is a chronic condition characterised by the relapsing inflammation despite previous endoscopic and histological healing. Our objective was to identify the molecular signature associated with UC remission.

Design We performed whole-genome transcriptional analysis of colonic biopsies from patients with histologically active and inactive UC, and non-inflammatory bowel disease (non-IBD) controls. Real-time reverse transcriptase-PCR and immunostaining were used for validating selected genes in independent cohorts of patients.

Results Microarray analysis (n=43) demonstrates that UC patients in remission present an intestinal transcriptional signature that significantly differs from that of non-IBD controls and active patients. Fifty-four selected genes were validated in an independent cohort of patients (n=30). Twenty-nine of these genes were significantly regulated in UC-in-remission subjects compared with non-IBD controls, including a large number of epithelial cell-expressed genes such as REG4, S100P, SERPINB5, SLC16A1, DEFB1, AQP3 and AQP8, which modulate epithelial cell growth, sensitivity to apoptosis and immune function. Expression of inflammation-related genes such as REG1A and IL8 returned to control levels during remission. REG4, S100P, SERPINB5 and REG1A protein expression was confirmed by immunohistochemistry (n=23).

Conclusions Analysis of the gene signature associated with remission allowed us to unravel pathways permanently deregulated in UC despite histological recovery. Given the strong link between the regulation of some of these genes and the growth and dissemination of gastrointestinal cancers, we believe their aberrant expression in UC may provide a mechanism for epithelial hyper-proliferation and, in the context of malignant transformation, for tumour growth.

Summary box

What is already known about this subject?

- In ulcerative colitis (UC), periods of active disease are followed by endoscopic remission and healing of the involved mucosa.
- The involved intestinal mucosa of UC patients in remission shows persistent histological changes suggesting that the composition and architecture of the recovered intestine is permanently altered even after inflammation has resolved.
- Patients with UC have an increased risk of developing complications such as colorectal cancer (CRC), fibrosis and loss of intestinal function, and this risk increases over time.

What are the new findings?

- We identify a new transcriptional signature associated with the involved mucosa of UC patients in remission that is significantly different from that of uninvolved or non-inflammatory bowel disease mucosa.
- About half of the genes that are significantly regulated in UC active mucosa remain altered during remission despite endoscopic and histological healing. These genes participate in biological functions such as cellular growth, movement, assembly and organisation, as well as in fatty acid and protein metabolism.
- Among the genes that remain deregulated during remission, we identify several that are expressed by epithelial cells and are involved in epithelial cell proliferation, resistance to apoptosis and response to stress. These genes have been previously shown to be deregulated in the neoplastic epithelium, suggesting a potential contribution to CRC development in the context of UC.

▶ http://dx.doi.org/10.1136/gutjnl-2012-303765

INTRODUCTION

Ulcerative colitis (UC) is an idiopathic chronic disease of the colon characterised by periods of active disease followed by periods of remission. Epidemiological studies in UC have reported that over 90% of patients have active disease during the first year following diagnosis and in subsequent years, approximately 50% will have active disease or will have undergone colectomy.[1]

Preventing disease relapse, achieving mucosal healing and avoiding complications are the major goals in the management of patients with UC. Mucosal healing or endoscopic remission is associated with better long-term clinical outcomes in UC.[2] However, even in the absence of endoscopic or microscopic signs of active inflammation, the involved intestinal mucosa of UC patients in remission shows histological changes. These include

Summary box

How might it impact on clinical practice in the foreseeable future?

- By comparing active UC patients with UC patients in remission, we can distinguish between genes whose expression pattern depends on disease activity, and those that remain altered in spite of remission. The former could serve as potential targets and be used as objective biomarkers of mucosal inflammation.
- The signature associated with the remitting intestine may include early biomarkers of malignant transformation in UC patients, and potential targets for halting the progression to CRC.

glandular deformity, branching of crypts, thickened muscularis mucosa, Paneth cell metaplasia, neuroendocrine cell hyperplasia and/or fat in the lamina propria, suggesting that the composition and architecture of the recovered intestine is permanently altered even after inflammation has resolved.[3]

UC is associated with a higher risk of developing dysplasia and colorectal cancer (CRC),[4 5] with disease duration being the strongest risk factor. The histological severity of inflammation has been linked to increased cancer risk, but patients with long-standing remission also have an increased risk of developing neoplastic lesions.[6]

While several studies have used genome-wide gene expression approaches to understand the mechanisms of active inflammation,[7–12] fewer studies, typically relying on a small number of patients, have explored the molecular events that occur during remission.[9 13 14]

The primary objective of our investigation was to reveal the molecular events that take place during disease quiescence. To this end, we studied the transcriptional signature of the involved intestinal mucosa of UC patients in clinical, endoscopic and histological remission, and compared it with that of the actively inflamed or healthy non-inflammatory bowel disease (non-IBD) mucosa. Studying the molecular alterations in the intestinal mucosa that persist during disease remission may help identify relevant biomarkers of remission and provide a better understanding of the mechanisms leading to long-term disease complications such as dysplasia and CRC.

MATERIALS AND METHODS

More detailed information is described in the online supplementary methods.

Patient population

Patients with an established diagnosis of UC and non-IBD controls were included in the study after obtaining written informed consent. Non-IBD controls were those subjects undergoing colonoscopy for mild gastrointestinal symptoms or a screening for CRC, and who presented no lesions during examination. Inclusion criteria for UC patients were: age between 18 and 65 years, and diagnosis of UC at least 6 months before inclusion according to the established criteria.[15] Patients with concomitant infections were excluded.

A total of 89 subjects, divided into three independent cohorts, were included in the study. Clinical and demographic characteristics of the subjects are shown in table 1.

Table 1 Clinical and demographic characteristics of patients included in the study

	UC active	UC remission	Non-IBD controls
COHORT 1 (microarray analysis)			
Number	15	8	13
Gender (M/F)	4/11	3/5	5/8
Age (years)	42.4±9.1	49.4±11.7	41.6±12.4
Duration of disease (years)	6.6±5.2	12.4±8.8	–
Extension of disease*	0/8/7	1/5/2	–
Medication†	4/8/1/2	5/3/0/0	–
COHORT 2 (Real-time RT-PCR)			
Number	8	12	10
Gender (M/F)	5/3	6/6	3/7
Age (years)	49.5±17.3	40.5±11.2	42.7±9.9
Duration of disease (years)	3.6±3.9	10.3±6.3	–
Extension of disease*	2/5/1	1/7/4	–
Medication†	3/1/1/3	2/5/0/5	–
COHORT 3 (immunohistochemistry analysis)			
Number	7	9	7
Gender (M/F)	5/2	7/2	2/5
Age (years)	48±17.9	58.6±14.3	45.6±19.5
Duration of disease (years)	6.3±6.6	11.4±5.4	–
Extension of disease*	0/4/3	2/3/4	–
Medication†	1/5/1/0	4/4/0/1	–

*Proctitis/Left-sided colitis/Pancolitis.
†5ASA/Azathioprine/Steroids/no treatment.
IBD, inflammatory bowel disease; UC, ulcerative colitis.

Assessment of disease activity

Clinical and histological disease activity was assessed using the total Mayo score,[16] and the Matts score,[17] respectively. A total Mayo score greater than or equal to 4 with at least one point in the bleeding sub-score and two points in the endoscopic sub-score, together with a histological score greater than or equal to 3 in any colonic segment, was defined as active disease. Inactive disease was defined as a Mayo score less than 4, an endoscopic sub-score of 0 and a histological score less than or equal to 2. All inactive patients had been in remission for at least 5 months before and after biopsy collection. Uninvolved mucosa of UC patients was defined as a colonic segment with a completely normal endoscopic appearance, normal histology and the absence of any evidence of previous disease activity.

Biopsy collection

Intestinal biopsies were collected from the sigmoid colon or rectum of non-IBD controls, UC patients with quiescent disease (involved mucosa segments; UC remission) and UC patients with active disease (UC active involved). In patients with active disease, additional samples were obtained from uninvolved proximal segments whenever possible (UC active uninvolved). Biopsies were taken during routine colonoscopies, placed in RNA later RNA Stabilisation Reagent (Qiagen) and stored at −80°C. None of the biopsies showed evidence of colitis-associated dysplasia or neoplasia.

RNA Isolation

Total RNA from biopsies in cohorts 1 and 2 was extracted using a Rneasy Kit (Qiagen, Spain) according to the manufacturer's instructions. Purity and integrity of the total RNA were assessed with the 2100 Bioanalyzer (Agilent, Germany) and then quantified by NanoDrop spectrophotometer (Nanodrop Technologies, USA); only samples with an RNA integrity number (RIN) greater than 7.0 were used.

Microarray

The derived cRNA from cohort 1 biopsies was hybridised to high-density oligonucleotide Affymetrix GeneChip Human Genome U133 Plus 2.0 Arrays (Affymetrix, USA) and raw data was analysed using Bioconductor tools in R (V.2.15.0). Pathway analysis using Ingenuity Pathways Analysis (IPA; Ingenuity Systems) was performed for those genes found to be significantly deregulated.

Microarrays raw data (.cel files) and processed data have been deposited in NCBI's Gene Expression Omnibus and are accessible through GEO Series accession number GSE38713 (http://www.ncbi.nlm.nih.gov/geo/query/acc.cgi?acc=GSE38713).

Quantitative real-time reverse transcriptase PCR (RT-PCR)

To validate the microarray data, we performed real-time RT-PCR analysis for a selected set of 54 target genes and 9 endogenous controls (see online supplementary table S1) from an independent cohort of 30 individuals (cohort 2) using custom designed TaqMan Low Density Arrays (TLDA platform, Applied Biosystems by Life Technologies, USA).

Microarray and real-time RT-PCR data correlation was assessed in a subset of 15 biopsies specimens obtained for microarray analysis (cohort 1) that was also analysed by real-time RT-PCR (7 UC remission, 4 UC active involved and 4 UC active uninvolved). We used Pearson's product moment correlation to test for any associations between paired data.

Immunostaining of intestinal samples

Using commercially available antibodies and the immunoperoxidase detection system, we determined the expression of REG4, REG1A, S100P and SERPINB5 (MASPIN) in paraffin-embedded sections from mucosa colonic biopsies obtained during endoscopies (cohort 3). Two blinded observers (NP and RMB) quantified the intensity of staining for all proteins analysed using a qualitative score ranging from 0 to 2 (0=negative stain, 1=mild stain, 2=strong stain). Statistical significance between groups was determined using Fisher's exact test.

Immunofluorescence staining was performed to confirm epithelial localisation of REG4, REG1A, S100P and SERPINB5 (MASPIN) in a subset of representative patients that were included in cohort 3. Epithelial cells were stained with an anti-EpCAM antibody.

Ethical considerations

The study was approved by the Institutional Ethics Committee of the Hospital Clinic of Barcelona (Spain) on March 2006 and was performed in accordance with the principles stated in the Declaration of Helsinki (updated October 1996).

RESULTS

The intestinal mucosa of UC in histological remission is transcriptionally different from that of healthy or inflamed mucosa

Our first aim was to compare, using microarray analysis, the transcriptional profile of the involved intestinal mucosa of patients in remission, with that of healthy or inflamed mucosa (cohort 1; table 1). A clear differentiation of samples, based on their inflammatory status, was evident when applying principal component analysis (PCA) using the given log2 microarray expression data (figure 1). Importantly, samples from involved areas of patients in remission (UC remission, shown in green in figure 1) clustered together and away from the other groups.

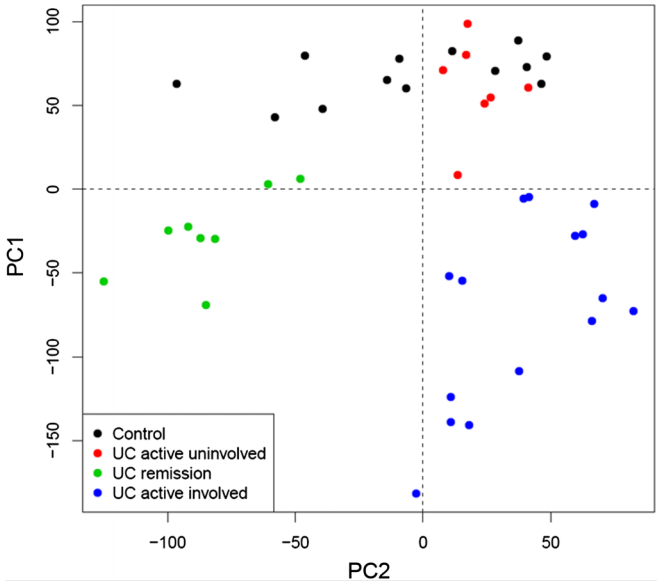

Figure 1 Principal Component Analysis (PCA) of microarray-based genome-wide gene expression profiles derived from intestinal biopsies. Mucosal biopsies were obtained from non-inflammatory bowel disease (non-IBD) controls (black, n=13), non-involved mucosa segments from patients with active ulcerative colitis (UC) (red, n=7), involved mucosa segments from patients with active UC (blue, n=15), and inactive UC (green, n=8). A two-principal component plot is shown with the first component along the Y-axis and the second component along the X-axis.

Using linear models for microarray data (LIMMA), we identified a set of 5469 genes whose expression was significantly up- or down-regulated in UC remission samples compared with non-IBD controls, thereby demonstrating that the UC mucosa in histological remission is distinguishable from that of non-IBD controls. By comparing inflamed samples from UC active patients with non-IBD controls, we identified 6365 genes that were significantly perturbed. It is worth noting that over half of those genes (3700) remained significantly deregulated in UC patients in remission despite complete endoscopic and histological healing. No significant differences in gene expression were detected in UC active uninvolved samples compared with non-IBD controls. Three different expression patterns could be identified by looking at the transcription of these 6,365 genes in UC remission samples relative to the other groups (figure 2). Pattern 1 included genes that showed equal expression in UC remission compared with non-IBD controls; pattern 2 contained genes whose expression in UC remission was intermediate and significantly different from that of controls and UC active; and pattern 3 included those genes that showed expression in UC remission comparable with that of UC active involved and was significantly different to non-IBD controls.

Analysis of the most significantly regulated pathways during UC remission based on transcriptomic data

Pathways analysis using IPA of the 3700 genes regulated in both active UC and UC in remission (patterns 2 and 3, figure 2) revealed several significantly perturbed biological functions (see online supplementary table S2A). The most noteworthy pathways identified included 945 of the 3700 genes (figure 3). A large share of these was related to fatty acid and protein metabolism. A decrease in biological functions linked to oxidation,

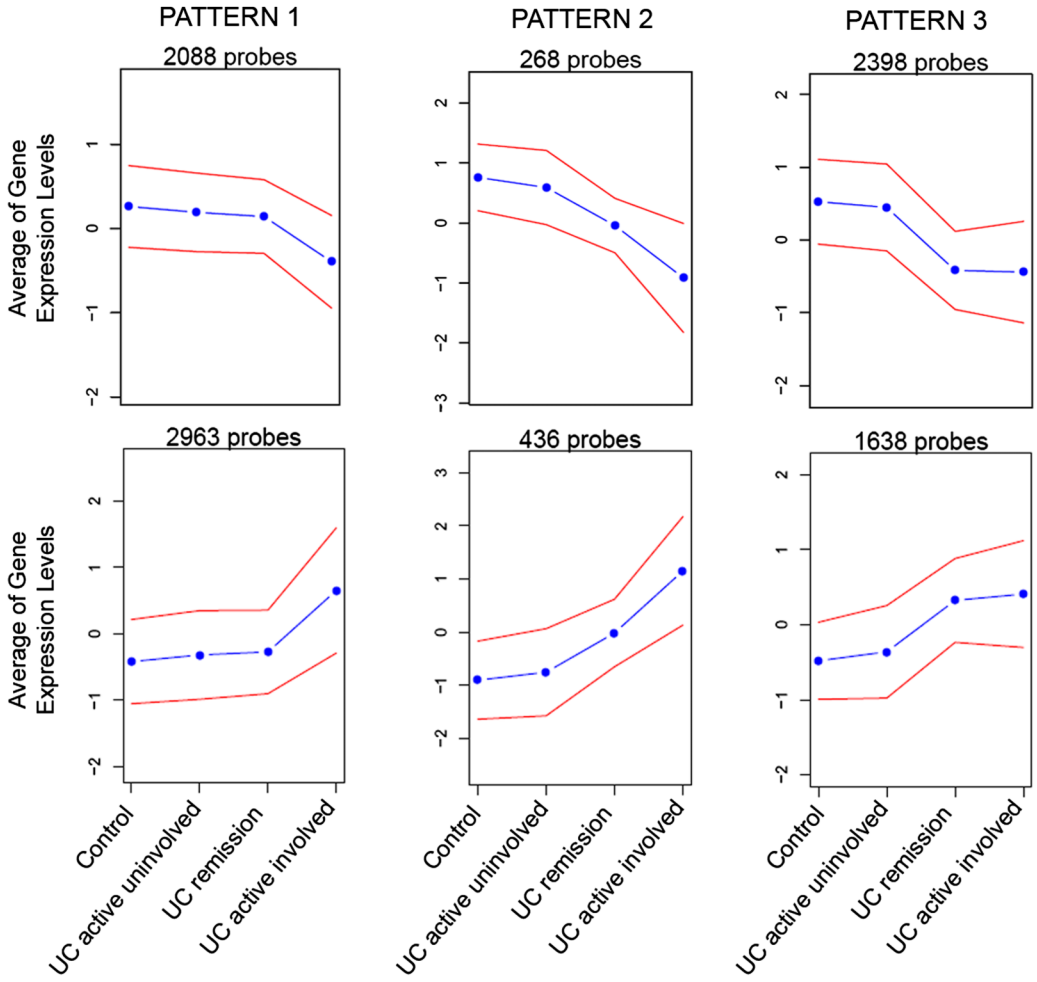

Figure 2 Expression patterns according to microarray analysis. The 6,365 genes identified as differential expressed between ulcerative colitis (UC) active and non-inflammatory bowel disease (non-IBD) controls were grouped into 6 clusters according to 3 expression patterns. For each cluster of genes, the average expression levels (blue points) and the corresponding SD (red line) are shown on the y-axis for each group of observations. The expression level of each gene was normalised to a mean=0.

concentration and transport of lipids is shown, suggesting reduced energy production, whereas protein metabolism increased. Pathway analysis also revealed a large number of regulated genes involved in cellular movement, mainly associated with the migration of cancer cells. Cellular assembly and organisation was perturbed, with a marked reduction in the tight junction and actin filament formation, and in the quantity of glandular epithelial cells. In addition, our analysis revealed an increase in the adhesion of stromal cells and in the spreading of fibroblasts during remission. Interestingly, biological functions related to colony formation and to the proliferation of colon cancer were found to be elevated. The cell death of epithelial cells and the cytotoxicity of tumour cells were similarly perturbed.

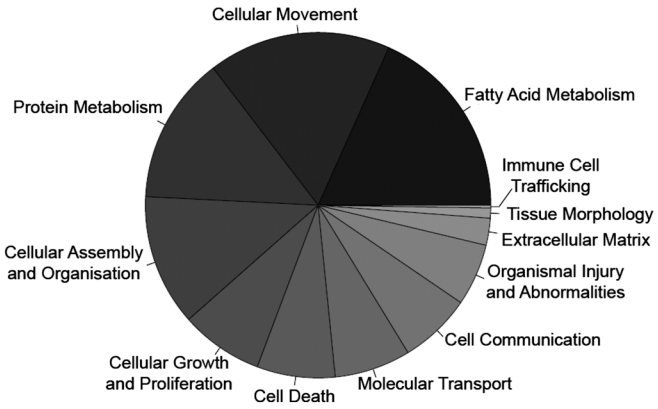

Figure 3 Pie chart representation of the relevant biological functions altered in both active ulcerative colitis (UC) and UC in remission. Twelve categories, including several biological functions, are shown across a range of black and white colouring.

By contrast, that set of genes exclusively deregulated in patients with active UC versus non-IBD controls (pattern 1, figure 2) was primarily associated with immune function and inflammatory response (immune cell trafficking, cell movement and communication, etc), though it was also found to play a role in proliferative and regenerative responses (cellular growth and proliferation, cell death and tissue morphology) (see online supplementary table S2B).

Identification of a UC in remission signature

We next selected 54 genes (see online supplementary table S1) that (1) belonged to one of the 3 aforementioned patterns of gene expression (figure 2) and that (2) were involved in some of the major regulated pathways discussed above. Figure 4 shows a

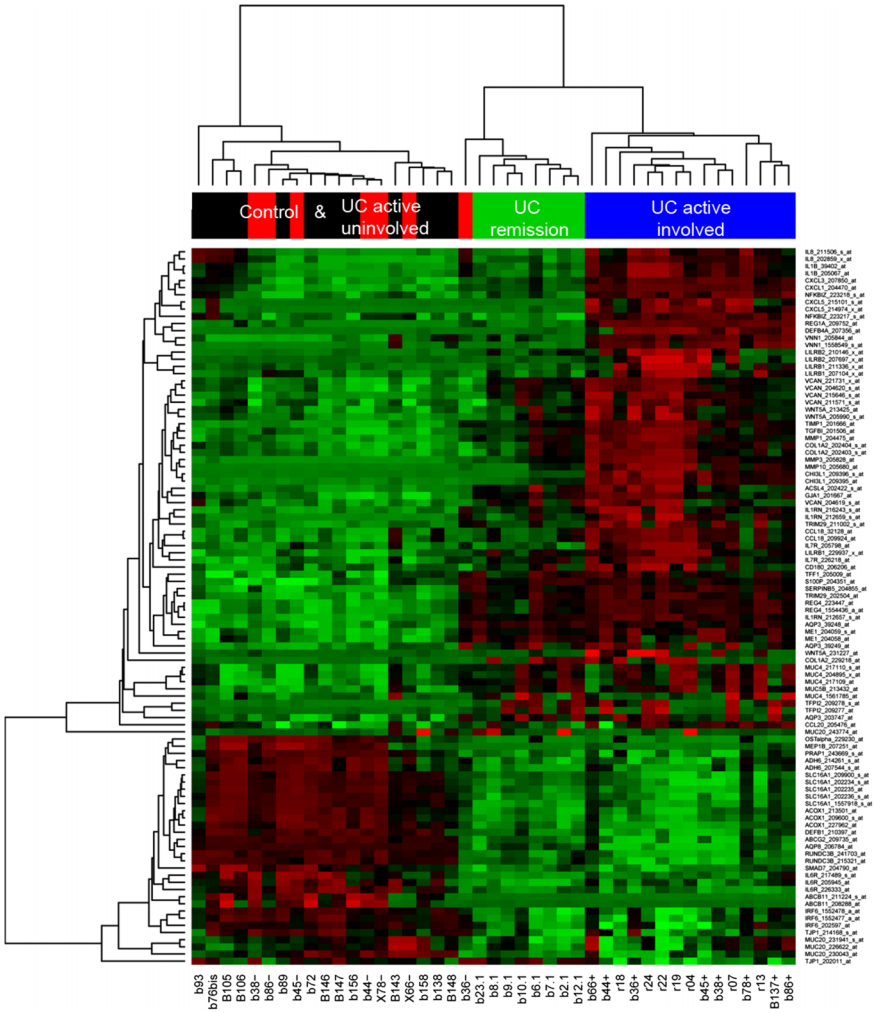

Figure 4 Heatmap representation of microarray expression of 54 candidate genes for the ulcerative colitis (UC)-in-remission signature (100 probes). Heatmap representation of microarray expression of 54 selected target genes. Each row shows one individual probe (representing 54 selected genes) and each column an experimental sample. High expression levels are shown in red and low expression levels in green. An unsupervised hierarchical cluster method, using a Pearson distance and average linkage method, was applied for each sample and gene classification. Samples belonged to one of the following groups: non-inflammatory bowel disease (non-IBD) controls (shown in black, n=13), non-involved mucosa segments from patients with active UC (UC active uninvolved; in red, n=7), involved mucosa segments from patients with active UC (UC active involved; in blue, n=15) and endoscopically and histologically inactive UC (UC remission; in green, n=8).

heatmap representation of the microarray expression profile for the chosen 54 genes (100 probes). Microarray expression values for these 54 genes allowed discrimination between groups of UC patients in an unsupervised hierarchical cluster analysis of samples from cohort 1 (figure 4). The selected genes included several belonging to pattern 1 (ie, REG1A, IL8, CXCL3 and WNT5A) shown in the upper part of the heatmap (figure 4), and genes whose expression was deregulated in UC remission and UC active involved samples compared with non-IBD controls (patterns 2 and 3). Ninety-six per cent of the genes selected (52 out of the 54 analysed) were technically validated by real-time RT-PCR. Correlation coefficients (r) between the expression of microarray and real-time RT-PCR analyses and the p values for each probe are shown in the online supplementary table S3.

The UC-in-remission signature is confirmed by real-time RT-PCR in an independent cohort of patients

Next, we analysed the expression of these 52 selected genes using real-time RT-PCR in an independent cohort of patients (cohort 2; table 1). We obtained a refined set of 38 genes (table 2) whose expression profile fell into one of the three patterns described above (figure 2). As expected, we identified a marked up-regulation in UC active involved samples of all pattern 1 selected genes. In particular, REG1A showed the highest up-regulation (1363.4-fold change compared with non-IBD controls and a 403.4 fold-change compared with UC remission samples), followed by IGHG1, IL8, CXCL1 and CXCL3. The pattern 2 genes CHI3L1, MMP1, MMP3 and TIMP1, which are related to the extracellular matrix, showed a marked up-regulation both in UC active and in UC remission samples compared with controls. By contrast, AQP8, a transporter found in the apical membrane of enterocyte cells (pattern 2), was significantly down-regulated in UC active involved and UC remission samples. An additional 22 genes belonging to expression pattern 3 were validated in this cohort. These genes showed a significant up- or down-modulation in UC active involved and UC remission samples. For all pattern 3 genes, no significant differences were found between UC active and UC remission expression. Regenerating islet-derived family member 4 (REG4), an epithelial cell-growth factor, showed the highest up-regulation followed by SERPINB5, which was also expressed by epithelial cells. The relative expression of genes encoding for different epithelial cell transporters, such as ABCG2, AQP3 and SLC16A1, is also shown.

The expression of a subset of epithelial genes and proteins remains in a deregulated state during remission

Using patients in cohort 2, we validated a total of 29 genes as being differentially expressed in UC in remission compared with non-IBD controls (table 2, patterns 2 and 3). Remarkably, many of the genes (i.e. ABCG", AQP3, DEFB1, REG4, S100P, SLC16A1, TFF1, SERPINB5 (MASPIN), AQP8, TRIM29, RUNDC3B AND CHI3L1) whose transcription remained

Table 2 Changes in the expression of selected genes assessed by real-time RT-PCR

Gene symbol	Fold change		
	UC active involved versus control	UC remission versus control	UC active involved versus UC remission
Pattern 1			
COL1A2	7.0**	1.1	6.3**
CXCL1	21.1**	1.9	11.1**
CXCL3	11.5**	1.9	6.0*
IGHG1/G4/@/G3/V4–31/M	59.5**	1.3	44.1*
IL8	29.6**	1.6	18.1*
NFKBIZ	2.9**	1.1	2.8**
REG1A	1363.4**	3.4	403.4**
VCAN	3.9**	−1.1	4.4*
WNT5A	5.1**	−1.1	5.7**
Pattern 2			
AQP8	−59.8**	−9.4**	−6.3*
CHI3L1	626.0**	12.3**	50.9**
LILRB2	7.3**	1.8*	4.0*
MMP1	111.8**	13.8**	8.1*
MMP3	354.8**	22.6**	15.7*
TGFBI	5.9**	2.0**	2.9*
TIMP1	10.9**	4.0**	2.8*
Pattern 3			
ABCG2	−8.3**	−4.7*	−1.8
ACOX1	−2.2**	−1.9**	−1.1
ACSL4	6.1**	2.4**	2.6
ADH6	−2.3*	−1.7*	−1.4
AQP3	3.1**	4.0**	−1.3
CXCL5	44.7**	3.9*	11.5
DEFB1	−3.3**	−1.9*	−1.7
GJA1	4.2**	2.1**	2
IL1B	18.7**	2.6*	7.1
IL1RN	12.7**	7.9**	1.6
IL6R	−1.7*	−1.4*	−1.2
ME1	5.7**	6.6**	−1.2
MMP10	48.8**	10.4**	4.7
REG4	25.1**	22.7**	1.1
RUNDC3B	−3.1*	−2.3*	−1.3
S100P	8.6**	13.0**	−1.5
SERPINB5	10.0**	15.2**	−1.5
SLC16A1	−3.5*	−2.9**	−1.2
SMAD7	−1.9**	−1.5*	−1.3
TFF1	9.7**	6.0**	1.6
TFPI2	13.3**	6.3**	2.1
TRIM29	7.9**	9.8**	−1.3

*p<0.05.
**p<0.005.
Relative change (fold change) in gene expression determined by real-time RT-PCR in non-IBD controls, involved areas of active UC patients (UC active involved), and involved areas of UC patients in endoscopic remission (UC remission). Based on their relative expression among groups, genes could be classified into three different patterns (described in figure 2). Significant adjusted p values from a Mann-Whitney-Wilcoxon test are shown as.
IBD, inflammatory bowel disease; RT-PCR, reverse transcriptase PCR; UC, ulcerative colitis.

altered despite mucosal healing were primarily expressed by epithelial cells; this suggests that the epithelial lining is particularly susceptible during this chronic inflammatory condition.

Figure 5 shows the boxplot representation of gene expression by real-time RT-PCR for some of the most relevant epithelial cell-expressed genes that remained in a deregulated state in UC-in-remission samples. In addition, the expression of REG1A, a gene only up-regulated in UC active involved samples, is shown as a marker of inflammation. Apical membrane butyrate receptor (SLC16A1) and the molecular transporters (AQP8 and ABCG2), which are expressed primarily by enterocytes, showed a significant down-regulation both in active UC and UC in remission. By contrast, the expression of AQP3, a basolateral transporter of these cells, exhibited a significant increase in transcription. Two genes secreted by goblet cells, REG4 and TFF1, also showed an increase in transcription. Moreover, the expression of less well-known epithelial genes—such as S100P, SERPINB5, TRIM29, RUNDC3B and CHI3L1—remained significantly altered in UC in remission.

In order to further confirm this signature, we determined by immunohistochemistry the expression of 3 selected proteins: REG4, S100P and SERPINB5 (table 2). In addition, we determined the expression of REG1A (pattern 1, figure 2 and table 2) as an epithelial marker of ongoing inflammation. Intestinal epithelial localisation of all four antigens was confirmed by immunofluorescent co-staining with an epithelial marker (EpCAM). Expression of REG4, REG1A, S100P and SERPINB5 (shown in green) within EpCAM-positive (in red) intestinal epithelial cells in the intestinal crypts is shown in figure 6A (white arrows). Strong S100P-expressing cells negative for EpCAM were also identified in the intestinal lamina propria (figure 6A, yellow arrow).

Protein expression of these four epithelial-related genes was quantified by immunohistochemistry in a cohort of 23 patients (cohort 3; see table 1 for patients' characteristics). In all samples tested, the expression of REG1A, REG4 and SERPINB5 was localised exclusively to the intestinal epithelium, whereas both epithelial cells and a subset of lamina propria cells stained for S100P (figure 6B). As expected, non-IBD control samples showed negative or mild staining for REG4, S100P, SERPINB5 and REG1A, while these four proteins exhibited significantly increased expression in the inflamed mucosa of active UC patients (representative immunostainings are shown in figure 6B). The intensity for each protein was determined using a qualitative score ranging from 0 to 2 (0=negative stain, 1=mild stain, 2=strong stain). Expression of S100P and SERPINB5 was significantly higher in UC in remission ($p<0.04$) compared with controls, while the expression of REG4 did not reach statistical significance ($p=0.13$). In agreement with the transcriptional data (both microarray and real-time RT-PCR), expression of REG1A in UC-in-remission patients was comparable with non-IBD controls and significantly different ($p<0.005$) from that of the involved areas of UC active patients (figure 6C).

DISCUSSION

In the present study, we examined the transcriptional profile of the intestinal mucosa of UC patients in remission, using a whole-genome approach. Our study identified pathways that are permanently deregulated in UC despite endoscopic and histological remission.

During active inflammation, a large number of genes are significantly regulated in UC patients.[7–12] As is common in stressed tissues, this includes purely pro-inflammatory genes, and numerous protecting and regenerating mechanisms. Activation of these mechanisms of defense is essential to overcoming cellular stress. In fact, a failure to correctly do so can lead to more severe tissue damage and/or chronic inflammation. These protective mechanisms, which are induced as a response to stress, need to be turned off once the stressor (eg, infectious organism, damaging agent, etc) is eliminated in order to avoid, for instance, uncontrolled cell proliferation, which can lead to fibrosis or dysplasia. In the context of chronic inflammation

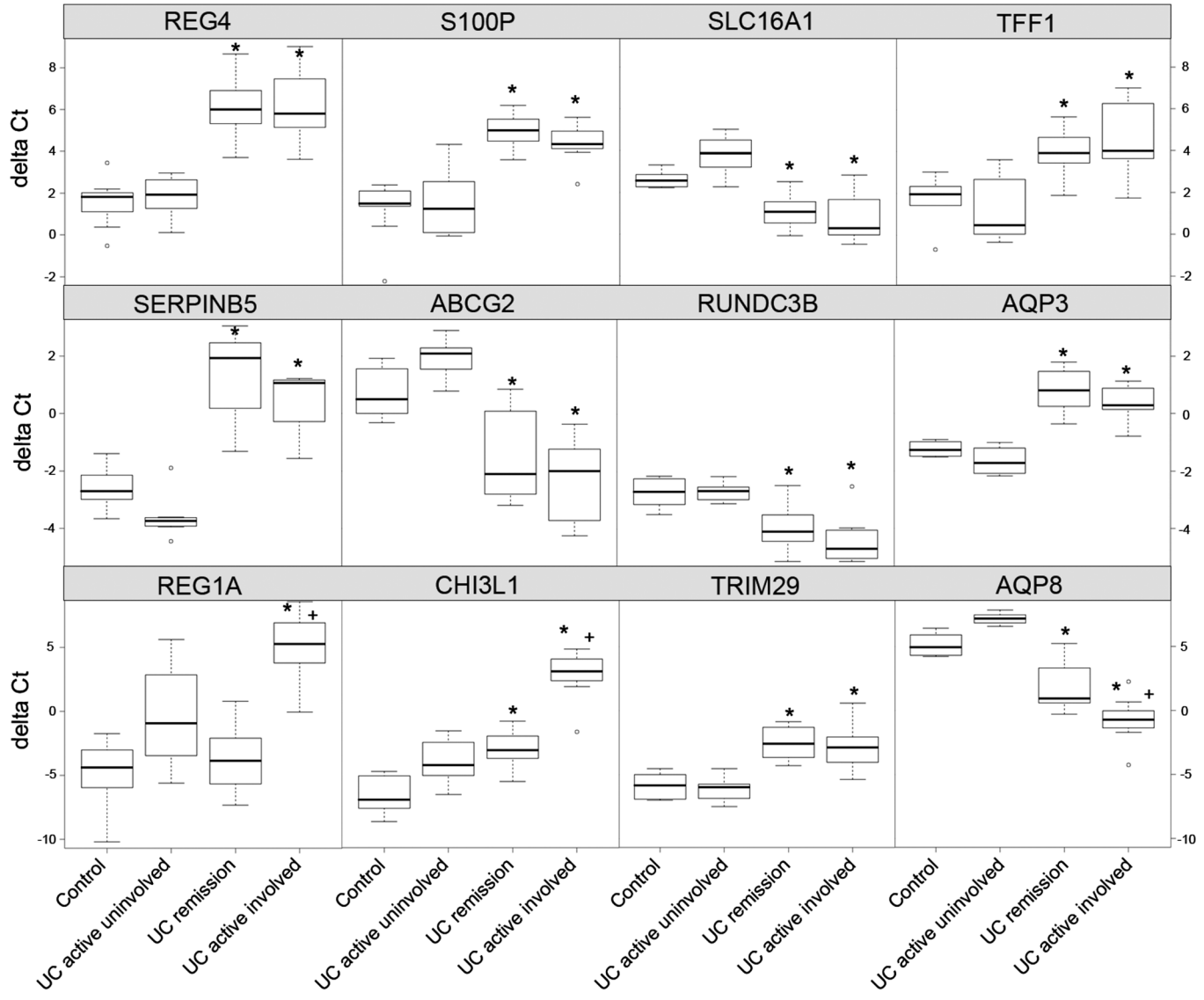

Figure 5 Expression of selected epithelial cells-expressed genes determined by real-time reverse transcriptase PCR (RT-PCR) in non-inflammatory bowel disease (non-IBD) controls and ulcerative colitis (UC) patients with active and inactive disease. Boxplot representation of 12 epithelial cell-expressed genes as measured by real-time RT-PCR (delta Ct) in cohort 2, including 10 non-IBD controls, 12 UC remission, 8 UC active uninvolved and 7 UC active involved samples. Statistical significance compared with controls (*$p<0.05$) and with UC in remission (+$p<0.05$) is shown.

(UC), however, it remains unclear whether these genes, which belong to both pro-inflammatory and protective subsets, return to homeostatic levels once inflammation is under control.

As we and others,[9 12 13 18 19] have shown, remission can indeed be accomplished by modulating the inflammatory response with a large number of reversibly modulated genes capable of returning to basal levels. These include genes that transcribe for cytokines, adhesion molecules, immunoglobulins, antimicrobial peptides and tissue-remodelling enzymes, among many others. Achieving expression profiles for this gene set comparable with those seen in a healthy intestine appears to be necessary in order to completely heal the mucosa of UC patients. These genes (ie, IL8, REG1A and CXCL1) and the proteins they encode may therefore represent important targets whose modulation would be associated with mucosal healing and clinical recovery. Moreover, they may constitute good biomarkers that closely correlate with clinical, endoscopic and histological remission, as we have recently shown.[19] While this set of genes is reversely induced or repressed, a second group that is also significantly up- or down-regulated in active disease shows only partial or no modulation in inactive patients, despite complete histological and endoscopic remission. This suggests that modulation of this gene set is not required to achieve mucosal healing, and that—in contrast to the first set of reversibly modulated genes—these genes may not serve as candidate targets or biomarkers of disease activity. Overall, our data strongly suggests that the involved intestinal mucosa of UC patients does not return to "normal" after inflammation has resolved, but rather remains in a permanently altered state characterised by a unique transcriptional signature. Importantly, many of the genes we identified as being perturbed in UC-in-remission mucosa have been widely reported to be associated with the development of gastrointestinal carcinomas.[20–25] In particular, REG4, S100P and SERPINB5, three of the genes here associated with the inactive UC signature, are known to be involved in epithelial cell proliferation and

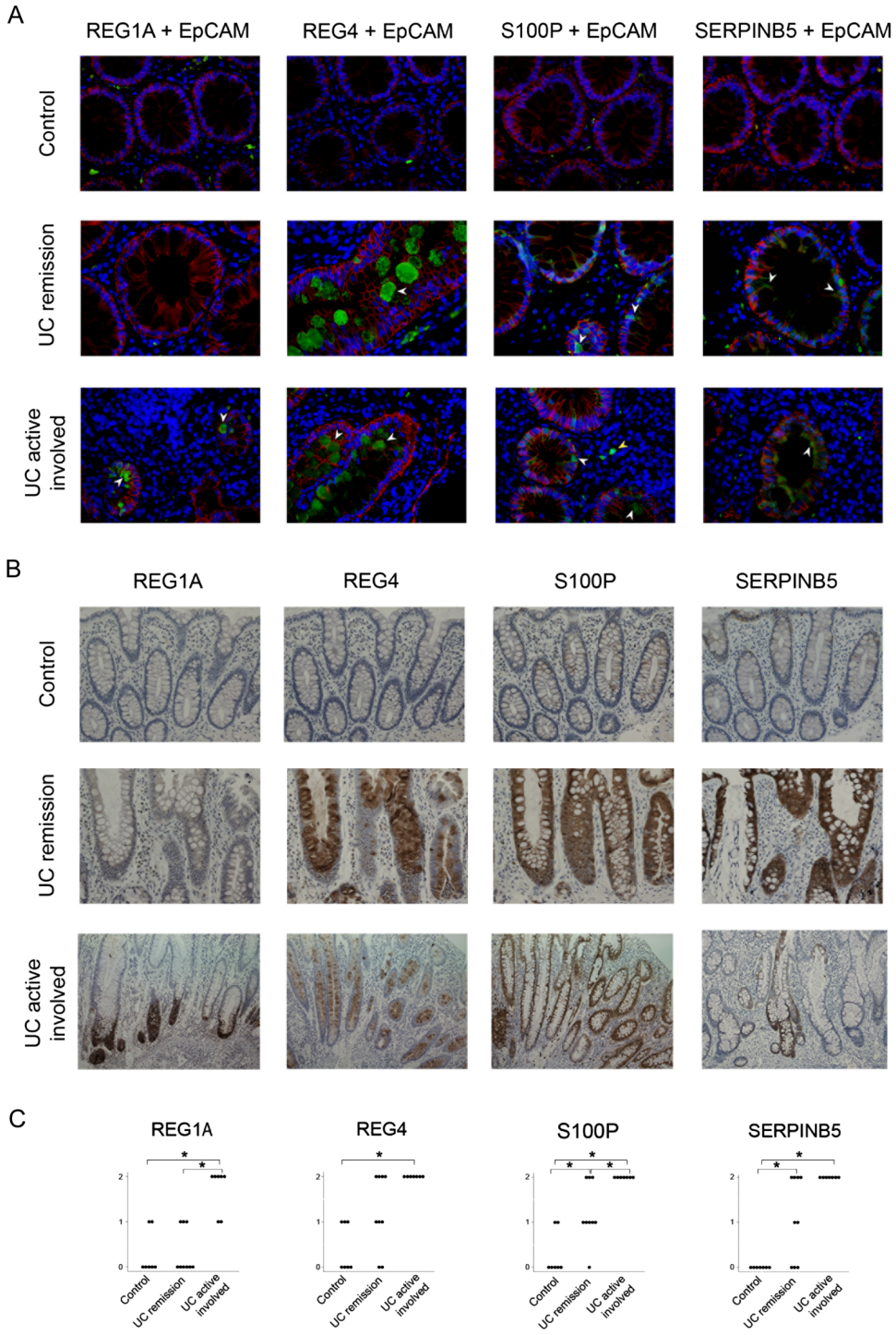

Figure 6 Immunostaining of REG1A, REG4, S100P and SERPINB5 in epithelial cells shows different intensity patterns in active ulcerative colitis (UC) or UC in remission and non-inflammatory bowel disease (non IBD) control biopsy samples. (A) Representative two-colour immunofluorescent staining of fixed paraffin-embedded colonic tissue from one non-IBD control, one UC-in-remission patient (involved mucosa), and from an active UC (UC active involved) patient. All samples were co-stained with EpCAM (red) and one of the following selected markers: REG1A, REG4, S100P or SERPINB5 (green). Sections were counterstained with DAPI (blue). Images were obtained using a 40x objective. White arrows highlight co-localisation of proteins. The yellow arrow shows S100P expression by non-epithelial cells. (B) Representative immunohistochemical staining of fixed paraffin-embedded colonic tissue from one non-IBD control, from the involved area of a patient with endoscopically and histologically inactive UC (UC in remission), and from a patient with active UC (UC active involved). All samples were stained with REG1A, REG4, S100P and SERPINB5 antibodies. Sections were counterstained with haematoxylin. Images from the non-IBD control and the UC remission patient were taken with a 20x objective lens, while the UC active involved subject image was obtained using a 10x objective lens in order to view the whole crypt length. (C) Scatterplot representation of qualitative scores for REG1A, REG4, S100P and SERPINB5 immunohistochemical staining in a cohort of 23 patients (non-IBD controls, n=7; inactive UC (UC remission), n=9; active UC (UC active involved), n=7). Each black dot represents one individual sample. Staining scores range between 0 and 2 (0=negative stain, 1=mild stain, 2=strong stain) for all proteins. Statistical significance between groups was determined using Fisher's exact test and is represented as *p<0.05.

resistance to apoptosis. REG4 is the most recently described member of the regenerating C-type lectin family of proteins.[26] REG4 promotes cell growth by inducing the expression of the anti-apoptotic genes BCL-2, BCL-X and Survivin,[27] and its transcription is induced by different growth factors.[28] By contrast, expression of the genes that encode for other family members, such as REG1A and REG3, is induced in response to pro-inflammatory cytokines such as TNF-α, IL-6, IL-8, IFN-γ or IL-1β,[28 29] and as we show here, is significantly down-regulated during remission.

S100P belongs to the S100 family of proteins (which includes S100A8/S100A9, also known as calprotectin, a widely used faecal biomarker of disease activity in UC). This family of proteins is involved in the regulation of cell-cycle progression and differentiation. Similar to REG4, S100P is frequently over-expressed in several epithelial tumour types, including CRC.[24] Interestingly, a recent study reported the over-expression of S100P in both UC-associated high-grade dysplasia and colon cancer, and in the non-dysplastic mucosa of UC patients who progressed to dysplasia.[30] These findings suggest that there are changes in protein expression early in the neoplastic progression, before any histological changes become evident in epithelial cells.

SERPINB5 (MASPIN) is an intracellular serine protease inhibitor. Expression of SERPINB5 has been shown to gradually increase from non-cancerous mucosa to adenocarcinoma through adenoma.[31] SERPINB5 expression reportedly increased in over 90% of patients with active IBD, compared with 10% of healthy controls. In inactive chronic IBD, expression was seen in about 40% of patients,[32] in close agreement with our own results.

Importantly, our validated UC-in-remission signature included other epithelial cell-related genes including defensin DEFB1, SLC16A1 encoding for the butyrate receptor, the aquaporins AQP3 and AQP8, the trefoil factor TFF1, and those genes encoding for less well-known proteins such as TRIM29 and RUNDC3B. DEFB1 encodes for the antimicrobial peptide defensin β 1, which is constitutively expressed in the intestinal epithelium.[33] Defensins are key effectors of the innate immune response in the intestine. A decrease in expression of DEFB1 has been shown in colonic Crohn's disease, but not in UC.[33] Using larger cohorts of patients, both we and others,[14] have shown that DEFB1 is indeed significantly down-regulated in active UC and in recovered inactive patients, compared with non-IBD controls. Defective production of antimicrobial peptides could potentially lead to activation of the mucosal immune system and to promotion of disease relapse.

Another interesting target identified in this study is the SLC16A1 gene encoding for the butyrate receptor. Butyrate is a product of commensal metabolism and provides about 70% of the total energy requirements of colonocytes. A reduction in expression of the butyrate receptor during active UC has been previously reported to result in decreased butyrate oxidation.[34 35] Apart from being a source of energy for colonocytes, butyrate is involved in the inhibition of several key processes, such as colonic carcinogenesis, inflammation and oxidative stress. A decrease in SLC16A1 in intestinal epithelial cell lines reduces the intracellular availability of butyrate, thereby potentially affecting its oxidation and its regulatory effects on cell proliferation, differentiation, apoptosis and inflammation.[36–39] Therefore, lower SLC16A1 expression might promote uncontrolled epithelial cell proliferation and contribute to the risk of CRC development. Indeed, SLC16A1 expression is down-regulated dramatically during colon carcinogenesis. This down-regulation of SLC16A occurs as a relatively early event in the adenoma-carcinoma sequence.[25]

In summary, using transcriptional analysis of the intestinal mucosa we describe herein a unique molecular signature associated with UC in remission. By showing that this gene set is being aberrantly expressed in remitting UC mucosa, we believe the evidence points to new molecular mechanisms that potentially become perturbed in the involved mucosa of UC patients in remission. Interestingly, this signature closely resembles that of the malignantly transformed epithelium. The important question to answer is whether permanent deregulation of these genes influences long-term UC-associated complications such as epithelial cell transformation, loss of intestinal function and disease relapse. While we cannot conclude from our study what the physiological consequences of maintaining these genes in a permanently perturbed state are, one can speculate that in the absence of active inflammation (in the remitting mucosa), the continued aberrant expression of these genes may facilitate the growth of spontaneously occurring malignant epithelial cells and/or promote disease relapse. Whether any of these genes could serve as reliable predictors of progression to CRC in UC patients requires further study.

Acknowledgements We thank the Endoscopy Department at Hospital Clinic Barcelona for providing us with the samples required to conduct this study, and our patients for their selfless participation. We are indebted to Dr Daniel Benitez-Ribas, Dr Elisabeth Calderón-Gómez, and Dr Isabella Dotti for their critical reading of the manuscript and to Joe Moore for the editorial assistance.

Competing interests None.

Contributors AS and JP designed the study; MCM, IO and ER recruited patients; IO and ER assessed clinical disease activity; MJ assessed histological disease activity; NP, RMB and ME performed experiments; NP and JJL performed bioinformatic and biostatistic analysis; and AS, NP, JMP and JP wrote the manuscript.

Funding This work was supported by grant BFU2008–02 683/BFI to AS from the Ministerio de Ciencia e Innovación, Spain, and by CIBERehd.

Ethics approval Hospital Clínic Ethical Committee.

Provenance and peer review Not commissioned; externally peer reviewed.

Data sharing statement Microarray raw data from samples included in this study have been deposited in NCBI's Gene Expression Omnibus and are accessible through GEO Series accession number GSE38713.

REFERENCES

1. **Langholz E,** Munkholm P, Davidsen M, *et al*. Course of ulcerative colitis: analysis of changes in disease activity over years. *Gastroenterology* 1994;**107**:3–11.
2. **Colombel JF,** Rutgeerts P, Reinisch W, *et al*. Early mucosal healing with infliximab is associated with improved long-term clinical outcomes in ulcerative colitis. *Gastroenterology* 2011;**141**:1194–201.
3. **Ogra PL,** Mestecky J, Lamm ME, *et al*. *Mucosal immunology*. San Diego; Academic Press, 1999.
4. **Eaden JA,** Abrams KR, Mayberry JF. The risk of colorectal cancer in ulcerative colitis: a meta-analysis. *Gut* 2001;**48**:526–35.
5. **Rutter MD,** Saunders BP, Wilkinson KH, *et al*. Thirty-year analysis of a colonoscopic surveillance program for neoplasia in ulcerative colitis. *Gastroenterology* 2006;**130**:1030–8.
6. **Farraye FA,** Odze RD, Eaden J, *et al*. AGA technical review on the diagnosis and management of colorectal neoplasia in inflammatory bowel disease. *Gastroenterology* 2010;**138**:746–74, 774 e741–44; quiz e712–43.
7. **Lawrance IC,** Fiocchi C, Chakravarti S. Ulcerative colitis and Crohn's disease: distinctive gene expression profiles and novel susceptibility candidate genes. *Hum Mol Genet* 2001;**10**:445–56.
8. **Dieckgraefe BK,** Stenson WF, Korzenik JR, *et al*. Analysis of mucosal gene expression in inflammatory bowel disease by parallel oligonucleotide arrays. *Physiol Genomics* 2000;**4**:1–11.
9. **Noble CL,** Abbas AR, Cornelius J, *et al*. Regional variation in gene expression in the healthy colon is dysregulated in ulcerative colitis. *Gut* 2008;**57**:1398–405.
10. **Okahara S,** Arimura Y, Yabana T, *et al*. Inflammatory gene signature in ulcerative colitis with cDNA macroarray analysis. *Aliment Pharmacol Ther* 2005;**21**:1091–7.
11. **Costello CM,** Mah N, Häsler R, *et al*. Dissection of the inflammatory bowel disease transcriptome using genome-wide cDNA microarrays. *PLoS Med* 2005;**2**:771–87.
12. **Wu F,** Dassopoulos T, Cope L, *et al*. Genome-wide gene expression differences in Crohn's disease and ulcerative colitis from endoscopic pinch biopsies: insights into distinctive pathogenesis. *Inflamm Bowel Dis* 2007;**13**:807–21.

13. **Bjerrum JT,** Hansen M, Olsen J, *et al*. Genome-wide gene expression analysis of mucosal colonic biopsies and isolated colonocytes suggests a continuous inflammatory state in the lamina propria of patients with quiescent ulcerative colitis. *Inflamm Bowel Dis* 2010;**16**:999–1007.
14. **Arijs I,** De Hertogh G, Lemaire K, *et al*. Mucosal gene expression of antimicrobial peptides in inflammatory bowel disease before and after first infliximab treatment. *PLoS One* 2009;**4**:e7984.
15. **Stange EF,** Travis SP, Vermeire S, *et al*. European evidence-based Consensus on the diagnosis and management of ulcerative colitis: Definitions and diagnosis. *J Crohns Colitis* 2008;**2**:1–23.
16. **Schroeder KW,** Tremaine WJ, Ilstrup DM. Coated oral 5-aminosalicylic acid therapy for mildly to moderately active ulcerative colitis. A randomized study. *N Engl J Med* 1987;**317**:1625–9.
17. **Matts SG.** The value of rectal biopsy in the diagnosis of ulcerative colitis. *Q J Med* 1961;**30**:393–407.
18. **Olsen J,** Gerds TA, Seidelin JB, *et al*. Diagnosis of ulcerative colitis before onset of inflammation by multivariate modeling of genome-wide gene expression data. *Inflamm Bowel Dis* 2009;**15**:1032–8.
19. **Roman J,** Planell N, Lozano JJ, *et al*. Evaluation of responsive gene expression as a sensitive and specific biomarker in patients with ulcerative colitis. *Inflamm Bowel Dis* Published Online First: 12 May 2012. doi: 10.1002/ibd.23020
20. **Kamarainen M,** Heiskala K, Knuutila S, *et al*. RELP, a novel human REG-like protein with up-regulated expression in inflammatory and metaplastic gastrointestinal mucosa. *Am J Pathol* 2003;**163**:11–20.
21. **Oue N,** Kuniyasu H, Noguchi T, *et al*. Serum concentration of Reg IV in patients with colorectal cancer: overexpression and high serum levels of Reg IV are associated with liver metastasis. *Oncology* 2007;**72**:371–80.
22. **Glebov OK,** Rodriguez LM, Soballe P, *et al*. Gene expression patterns distinguish colonoscopically isolated human aberrant crypt foci from normal colonic mucosa. *Cancer Epidemiol Biomarkers Prev* 2006;**15**:2253–62.
23. **Birkenkamp-Demtroder K,** Olesen SH, Sorensen FB, *et al*. Differential gene expression in colon cancer of the caecum versus the sigmoid and rectosigmoid. *Gut* 2005;**54**:374–84.
24. **Fuentes MK,** Nigavekar SS, Arumugam T, *et al*. RAGE activation by S100P in colon cancer stimulates growth, migration, and cell signaling pathways. *Dis Colon Rectum* 2007;**50**:1230–40.
25. **Lambert DW,** Wood IS, Ellis A, *et al*. Molecular changes in the expression of human colonic nutrient transporters during the transition from normality to malignancy. *Br J Cancer* 2002;**86**:1262–9.
26. **Rafa L,** Dessein AF, Devisme L, *et al*. REG4 acts as a mitogenic, motility and pro-invasive factor for colon cancer cells. *Int J Oncol* 2010;**36**:689–98.
27. **Bishnupuri KS,** Luo Q, Sainathan SK, *et al*. Reg IV regulates normal intestinal and colorectal cancer cell susceptibility to radiation-induced apoptosis. *Gastroenterology* 2010;**138**:616–26, 626 e611–12.
28. **Nanakin A,** Fukui H, Fujii S, *et al*. Expression of the REG IV gene in ulcerative colitis. *Lab Invest* 2007;**87**:304–14.
29. **Sekikawa A,** Fukui H, Fujii S, *et al*. Possible role of REG Ialpha protein in ulcerative colitis and colitic cancer. *Gut* 2005;**54**:1437–44.
30. **Brentnall TA,** Pan S, Bronner MP, *et al*. Proteins That Underlie Neoplastic Progression of Ulcerative Colitis. *Proteomics Clin Appl* 2009;**3**:1326.
31. **Zheng H,** Tsuneyama K, Cheng C, *et al*. Maspin expression was involved in colorectal adenoma-adenocarcinoma sequence and liver metastasis of tumors. *Anticancer Res* 2007;**27**:259–65.
32. **Cao D,** Wilentz RE, Abbruzzese JL, *et al*. Aberrant expression of maspin in idiopathic inflammatory bowel disease is associated with disease activity and neoplastic transformation. *Int J Gastrointest Cancer* 2005;**36**:39–46.
33. **Peyrin-Biroulet L,** Beisner J, Wang G, *et al*. Peroxisome proliferator-activated receptor gamma activation is required for maintenance of innate antimicrobial immunity in the colon. *Proc Natl Acad Sci USA* 2010;**107**:8772–7.
34. **De Preter V,** Arijs I, Windey K, *et al*. Impaired butyrate oxidation in ulcerative colitis is due to decreased butyrate uptake and a defect in the oxidation pathway. *Inflamm Bowel Dis* 2012;**18**:1127–36.
35. **Thibault R,** De Coppet P, Daly K, *et al*. Down-regulation of the monocarboxylate transporter 1 is involved in butyrate deficiency during intestinal inflammation. *Gastroenterology* 2007;**133**:1916–27.
36. **Inan MS,** Rasoulpour RJ, Yin L, *et al*. The luminal short-chain fatty acid butyrate modulates NF-kappaB activity in a human colonic epithelial cell line. *Gastroenterology* 2000;**118**:724–34.
37. **Segain JP,** Raingeard de la Bletiere D, Bourreille A, *et al*. Butyrate inhibits inflammatory responses through NFkappaB inhibition: implications for Crohn's disease. *Gut* 2000;**47**:397–403.
38. **Siavoshian S,** Segain JP, Kornprobst M, *et al*. Butyrate and trichostatin A effects on the proliferation/differentiation of human intestinal epithelial cells: induction of cyclin D3 and p21 expression. *Gut* 2000;**46**:507–14.
39. **Cuff M,** Dyer J, Jones M, *et al*. The human colonic monocarboxylate transporter Isoform 1: its potential importance to colonic tissue homeostasis. *Gastroenterology* 2005;**128**:676–86.

Planell N et al. Supplementary Methods

MATERIALS AND METHODS

Microarray data analysis

Microarray raw data was analyzed using Bioconductor tools in R (www.r-project.org). The CG content-adjusted robust multi-array (GC-RMA) algorithm, which computes expression values based on probe intensity values that incorporate probe sequence information, was applied to Affymetrix raw data files in order to normalize them, resulting in a log2 expression value for each probe set. We then employed a conservative probe-filtering step, excluding those probe sets that failed to reach a log2 expression value of 5 in at least 1 sample, which resulted in the selection of a total of 22,206 probe sets out of the original 54,675. Principal component analysis of the given log2 microarray expression data matrix was carried out using basic tools in R (prcomp). Differential expression analysis was assessed by using linear models for microarray data (LIMMA), based on empirical Bayes moderated t-statistics for all filtered probe sets (22,206 probe sets). In addition, F-statistics were used to test for any change in expression over comparisons. To correct for multiple testing, the false discovery rate (FDR) was estimated from p-values derived from the moderated *t*-statistics using the method of Benjamini and Hochberg. Expression values were Z-transformed and empirical bayesian statistics and fold change were stored in an AFM-macro excel file. Genes were considered significantly up- or down-regulated if they had a p-value < 0.02 (FDR-adjusted empirical Bayes (LIMMA), FDR < 0.05) and at least a 1.5-fold variation in mean expression (log2 fc > |0.5849|).

Pathway analysis

Pathway analysis was performed for those genes significantly regulated ($p<0.02$; $FDR<0.05$; log2 fc > |0.5849|) in the affected colonic biopsies from active UC patients compared to non-IBD controls or patients in remission, using Ingenuity Pathways Analysis (Ingenuity™ Systems, www.ingenuity.com). Functional Analysis identified the biological functions and/or diseases that were most significant to the data set. Genes from the dataset that met the cut-off and that were associated with biological functions and/or diseases in the Ingenuity Pathways Knowledge Base were considered for analysis. Fischer's exact test was used to calculate a p-value for determining the probability that each biological function and/or disease assigned to that data set was due to chance alone. Genes whose expression was differentially regulated to a significant degree were overlaid onto a global molecular network developed from information contained in the Ingenuity Pathways Knowledge Base. Networks of these focus genes were then algorithmically generated based on their connectivity.

Quantitative real-time RT-PCR

Total RNA (1 μg) was transcribed to cDNA using reverse transcriptase (High Capacity cDNA Archive RT kit, Applied Biosystems). PCR was performed in TaqMan Universal PCR Master Mix (Applied Biosystems) according to the manufacturer's instructions. Fluorescence was detected in an ABI PRISM 7900 HT Fast Real-Time PCR System (Applied Biosystems). RealTime StatMiner software (Integromics) was used to calculate the cycle threshold (Ct).

Quantitative Real-Time RT-PCR Data Analysis

Real-time RT-PCR raw data was analyzed using Bioconductor tools in R statistical environment. In order to normalize Ct values the DeltaCts (ΔCt = Ct mean of reference gene – Ct target gene) were calculated using two endogenous control genes, UBA3 (ubiquitin-like modifier activating enzyme 3) and RPS3A (ribosomal protein S3A), selected by the Vandesompele method[1]. Missing expression data was imputed using the k-nearest neighbors method on Delta Ct values[2]. A non-parametric Kruskal-Wallis test and a Mann-Whitney-Wilcoxon test were done to examine statistically different expression patterns between groups. To correct for multiple testing, the method of Benjamini and Hochberg was used. An adjusted p-value of <0.05 was considered statistically significant.

Immunostaining of intestinal samples

Paraffin-embedded sections from mucosa colonic biopsies were pre-treated for deparaffinization, rehydration, and epitope retrieval using Dako EnVision Flex Target Retrieval Solution low pH (50x) in conjunction with PT Link (Dako, Glostrup, Denmark), with a warm step of 20 min at 95ºC, for immunohistochemical and dual immunofluorescent staining.

For immunohistochemical staining, sections were blocked with serum (Vectastain ABC kit; Vector Laboratories, USA) for 30 minutes and incubated overnight at 4ºC with commercially available antibodies: REG-IV polyclonal goat antibody (R&D Systems, USA; dilution 1:100), REG-1A polyclonal rabbit antibody (USBiological, USA; dilution 1:600), S100P polyclonal goat antibody (R&D Systems; dilution 1:200) and SERPINB5 monoclonal mouse antibody (BD Biosciences, USA; dilution 1:100). Sections were incubated with 3% H_2O_2 for 10 min in order to block peroxidase activity. Immunohistochemical staining was carried out using DAB chromogen (DAB, Sigma-Aldrich, St. Louis Missouri, USA) in the presence of a peroxidase enzyme (avidin/biotinylated enzyme complex, ABC). The sections were mounted with DPX Mountant for histology (Fluka) and examined with a Nikon Eclipse Ti microscope.

Dual immunofluorescent staining was performed following a simultaneous staining for EpCAM (monoclonal mouse anti-human EpCAM; 1:100, DakoCytomation, M0804) and REG4, REG1A or S100P, or a serial staining for EpCAM and SERPINB5.

For simultaneous staining, sections were blocked with 1% BSA for 30 minutes and incubated different mixtures of two primary antibodies: 1) anti-EpCAM and anti-REG-IV (2 hours at RT), 2) anti-EpCAM and anti-REG-1A (2 hours at RT), or 3) anti-EpCAM and anti-S100P (overnight at 4ºC). Donkey anti-mouse CY5 (Jackson Immunoresearch, Suffolk, UK), donkey anti-rabbit Alexa 488 (Invitrogen), and donkey anti-goat Alexa 488 (Invitrogen) were used as secondary antibodies. For serial staining, sections were blocked with 1% BSA for 30 minutes and incubated first with the primary (anti-SERPINB5, overnight at 4ºC) and secondary antibodies(Goat anti-mouse Alexa 488 (Invitrogen)), followed by a blocking step with 1% BSA for 30 minutes. Sections were then incubated with an anti-EpCAM mAb (2 hours at RT) followed by a secondary antibody (Donkey anti-mouse CY5).

Following immunostaining, all sections were mounted with Vectashield Mounting Medium with DAPI (Vector Laboratories) and examined with an Olympus DP72 microscope.

Regarding negative controls, specimens were processed under the same conditions in the absence of the corresponding primary antibodies.

REFERENCES

1. Vandesompele J, De Preter K, Pattyn K et al. Accurate normalization of real-time quantitative RT-PCR data by geometric averaging of multiple internal control genes. Genome Biol 2002; 3: 1-12.
2. Troyanskaya O, Cantor M, Sherlock G et al. Missing value estimation methods for DNA microarrays. Bioinformatics 2001; 17: 520-525.

Planell N et al. Supplementary Material

Supplementary Table 1. List of genes and probes validated by real-time RT-PCR or used as endogenous controls (*).

Assay ID	Gene Symbol	Gene Name
Hs00984887_g1	REG1A	regenerating islet-derived 1 alpha
Hs00175474_m1	DEFB4	defensin, beta 4
Hs01567913_g1	IL8	interleukin 8
Hs01555413_m1	IL1B	interleukin 1, beta
Hs00233987_m1	MMP10	matrix metallopeptidase 10 (stromelysin 2)
Hs00607029_g1	CXCL5	chemokine (C-X-C motif) ligand 5
Hs01011368_m1	CCL20	chemokine (C-C motif) ligand 20
Hs00268113_m1	CCL18	chemokine (C-C motif) ligand 18
Hs01072228_m1	CHI3L1	chitinase 3-like 1 (cartilage glycoprotein-39)
Hs01028971_m1	COL1A2	collagen, type I, alpha 2
Hs00605382_gH	CXCL1	chemokine (C-CX-C motif) ligand 1
Hs00171061_m1	CXCL3	chemokine (C-X-C motif) ligand 3
Hs00378230_g1	IGHG3	immunoglobulin heavy constant gamma 3 (G3m marker)
Hs00893626_m1	IL1RN	interleukin 1 receptor antagonist
Hs00902338_g1	IL7R	inteleukin 7 receptor
Hs00899660_g1	MMP1	matrix metallopeptidase 1 (interstitial collagenase)
Hs00968308_m1	MMP3	matrix metallopeptidase 3 (stromelysin 1, progelatinase)
Hs00944732_m1	NFKBIZ	nuclear factor of kappa light polypeptide gene enhancer in B-cells inhibitor, zeta
Hs01069973_m1	REG4	regenerating islet-derived family, member 4
Hs00932734_m1	TGFBI	transforming growth factor, beta-induced, 68kDa
Hs00355335_g1	TIMP1	TIMP metallopeptidase inhibitor 1
Hs01007937_m1	VCAN	veriscan
Hs01546812_m1	VNN1	vanin 1
Hs01086280_g1	AQP8	aquaporin 8
Hs01053787_m1	ABCG2	ATP-binding cassette, sub-family G (WHITE), member 2
Hs00380895_m1	OSTalpha	organic solute transporter alpha
Hs00376974_m1	PRAP1	proline-rich acidic protein 1
Hs00161826_m1	SLC16A1	solute carrier family 16, member 1
Hs00195535_m1	MEP1B	meprin A, beta
Hs00608345_m1	DEFB1	defensin, beta 1
Hs00289927_m1	RUNDC3B	RUN domain containing 3B
Hs01074241_m1	ACOX1	acyl-Coenzyme A oxidase 1, palmitoyl
Hs00184824_m1	ABCB11	ATP-binding cassette, sub-family B (MDR/TAP), member 11
Hs00167423_m1	ADH6	aclcohol dehydrogenase 6 (class V)
Hs00196213_m1	IRF6	interferon regulatory factor 6
Hs00416321_m1	MUC20	mucin 20, cell surface associated
Hs00998193_m1	SMAD7	SMAD family member 7
Hs00543824_m1	TJP1	tight junction protein 1 (zona occludens 1)
Hs00794121_m1	IL6R	interleukin 6 receptor
Hs00366414_m1	MUC4	mucin 4, cell surface associated
Hs01069872_m1	CD180	CD180 molecule
Hs01547083_m1	ACSL4	acyl-CoA synthetase long-chain family member 4
Hs00185020_m1	AQP3	aquaporin 3 (Gill blood group)
Hs00861588_m1	MUC5B	mucin 5B, oligomeric mucus/gel-forming
Hs00170216_m1	TFF1	trefoil factor 1
Hs00275975_m1	LILRB2	leukocyte immunoglobulin-like receptor, subfamily B, member 2
Hs01848117_s1	LILRB1	leukocyte immunoglobulin-like receptor, subfamily B, member 1

Hs00195584_m1	S100P	S100 calcium binding protein P
Hs01554892_m1	ME1	malic enzime 1, NADP(+)-dependent, cytosolic
Hs00197918_m1	TFPI2	tissue factor pathway inhibitor 2
Hs00998537_m1	WNT5A	wingless-type MMTV integration site family, member 5A
Hs00748445_s1	GJA1	gap junction protein, alpha 1, 43kDa
Hs00232590_m1	TRIM29	tripartite motif-containing 29
Hs00985283_m1	SERPINB5	serpin peptidase inhibitor, clade B (ovalbumin), member 5
Hs00420895_gH	RPLP0*	ribosomal protein, large, P0
Hs03023880_g1	ACTB*	actin, beta
Hs03005117_g1	RPS2*	ribosomal protein S2
Hs00744842_sH	TUBA1B*	tubulin, alpha 1 b
Hs00181460_m1	PPIC*	peptidylproplyl isomerase C (cyclophilin C)
Hs00234368_m1	UBA3*	ubiquitin-like modifier activating enzime 3
Hs00828752_gH	RPS20*	ribosomal protein S20
Hs00832893_sH	RPS3A*	ribosomal protein S3A
Hs99999901_s1	18S*	Eukaryotic 18S rRNA

Planell N et al. Supplementary Material

Supplementary Table 2. Biological pathways analysis by IPA. Pathway analysis was performed for those genes significantly perturbed in affected colonic biopsies from UC active and UC-in-remission samples compared to non-IBD controls (Supplementary Table 2A) or in UC active involved compared to non-IBD controls (Supplementary Table 2B), using Ingenuity Pathways Analysis (Ingenuity™ Systems, www.ingenuity.com).

In bold are shown those genes that were included in the real-time RT-PCR validation set.

Supplementary Table 2A. Main biological functions significantly perturbed in deregulated genes in both active and inactive UC versus non-IBD controls (patterns 2 and 3 of gene expression, Figure 2).

Biological functions	**Genes**
Cell communication: attachment of cells, cell-cell contact, disassembly of focal adhesions, adhesion of connective tissue cells, formation of tight junctions	**SERPINB5**, SLC4A2, TGFB1, **TGFBI**, VCAM1, DSG2, ICAM2, ITGA2, ITGA6, PTEN, PTGER2, **TFPI2**, TGFA, TGM2, **VCAN**, DSP, JAM2, JAM3, **GJA1**, OCLN, PARD3, **TJP1**, TJP3
Cell death: cell death of epithelial cell lines, cytotoxicity of tumor cell lines, apoptosis of endothelial cells, apoptosis of vascular endothelial cells, apoptosis of microvascular endothelial cells	FAS, FOXO3, GATA6, HGF, ITSN1, KLF5, LUM, MAP3K5, MAPK14, PARP1, SERPINA1, **SERPINB5**, TGFB1, THBS1, TLR3, TNFRSF10A, TNFRSF10B, TNFRSF11B, TNFSF10, **ABCG2**, JUN, MAP2K6, MET, PEA15, TCF3, TCF4, TGFA, TGFB1I1, TICAM1, TICAM2, TNFRSF1B, TRIM27, **SMAD7**, TGFBR2
Cellular assembly and organization: organization of actin and cytoskeleton, quantity of centrosome, proliferation of peroxisomes, induction of filaments, induction of actin stress fibers, fusion of liposome, formation of actin bundles, development of cytoplasm, stabilization of plasma membrane,	ABCD3, AKAP1, AKAP2/PALM2-AKAP2, ANG, ANKRD27, COL18A1, CTNND1, GAS7, GDA, GJC1, GNA11, GNA13, GNAQ, GNAS, GNG12, HGF, IPO4, JAG1, LAMP1, LAMP2, LIMK2, MAP1B, MAP1LC3A, MMP2, STAT3, SYNPO, TESK2, TGFB1, **TGFBI**, TPM2, TUBB, TWF1, UTRN, VCAM1, VIL1, WASL, XIAP, ZYX, ACTN1, MYO1B, DCN, SMAD4, **SMAD7**, CALD1, **ACOX1**, **TJP1**, TJP3

remodeling of actin filaments	
Cellular growth and proliferation: proliferation of colon cancer cell lines, colony formation of tumor cell lines, proliferation of colon carcinoma cells	CADM1, CAV1, CLU, CTSD, E2F5, EDN1, EGFR, ELF3, ENO1, FOXA2, FOXO3, GADD45B, **GJA1**, HGF, HMGA1, IGFBP7, **IL6R**, IL6ST, IP6K2, IRS1, KLF4, KLF6, NDRG1, NEK6, NF1, RUNX2, SERPINA1, SLPI, **SMAD7**, SPARC, STEAP2, **TFF1**, TNFSF10, TRIM22, VIP, ZEB1, DAPK2, NEDD9, NR5A2, PAK1, PDLIM4, PECAM1, PLD1, PPARG, SDC2, SLC26A2, SLC26A3, TCF4, TGFA, TGFBR2
Cellular movement: invasion of cancer cells, migration of cancer cells, invasion of colon cancer cell lines	CXCL12, ITGA2, ITGA6, **SERPINB5**, TGFB1, TGFBR1, BSG, CD82, EGFR, TGFA, TGFBR2, FGFR1, TIMP3, **WNT5A**, ANPEP, CCDC88A, CD24, CD44, CD9, CDC25B, CDH11, CLDN3, EPHB4, GAB1, GAB2, GEM, **GJA1**, GJB1, IGF2, ITGAV, JAM3, JUN, JUP, LAMA5, LAMC1, LCN2, **LILRB1**, **MMP3**, RUNX2, RUNX3, **S100P**, SDC2, SDCBP, SERP1, SERPINA1, SERPINE2, SLC9A3R1, SMAD4, **SMAD7**, STAT3, STK38L, SYK, TAGLN, TCF3, TCIRG1, **TFF1**, TFF2, **TFPI2**, **TGFBI**, THBS1, **TIMP1**, **TJP1**, TNFSF10, VAV3, **VCAN**, VDR, WWTR1, XIAP
Extracellular matrix: ruffling of fibroblast cell lines, shape change of fibroblast cell lines, adhesion of stromal cells, cell spreading of fibroblast cell lines, blebbing of fibroblast cell lines	VCAM1, CDC42SE2, FAS, MARCKS, NF2, ROCK1, TNFRSF10B, ASAP1, CAST, DAB2, EFNA1, FLNA, FLNC, FN1, MET, PALLD, PTBP1, TGFB1I1, THBS1, TNIK, TSPAN7, VAV3, VCL, VIM, DIAPH1, INSR, NCK2, PTEN, RAB4A, AKAP12, ARHGEF11, FGD4, GNG12, ITGA6, MAPK14, ZAK
Fatty acid metabolism: synthesis of sterol and cholesterol, oxidation of lipids, accumulation of lipid, concentration of phospholipid, concentration of fatty acid, conversion of lipid, beta-oxidation of fatty acid, export of lipid, fatty acid metabolism,	**ABCB11**, ABHD5, ACACA, ACAT1, **ACOX1**, AQP7, **IL1RN**, INSIG1, INSR, PIK3C2B, PIK3CB, PON2, SLC36A1, SREBF2, SYK, **TIMP1**, UCP2, VIP, ABCD3, ACAA2, ACADM, ACADS, ACADSB, **ACOX2**, ACSL5, **ACSL4**, MMP12, **MMP3**, MSN, RXRB, STX12, ABCB1, ABCC6, ACAA1, ACBD3, ACOT4, ACOT8, ACOT9, ACSL3, ACSM3, ANXA1,

efflux of colesterol	**AQP8**, **ME1**, ME3, SLC27A3
Immune cell trafficking: detachment of phagocytes	ANXA1, ANXA5, PTPRC, SIRPA
Molecular transport: secretion of hyaluronic acid, uptake of L-amino acid, import of protein, transport of oleic acid, transport of carbohydrate, uptake of essential amino acids, secretion of protein	AQP11, **AQP3**, AQP7, FABP1, INSR, IRS1, LYN, MAP4K4, SLC23A1, SLC35A3, SLC35B4, SLC37A4, ACSL3, **ACSL4**, ACSL5, SLC3A1, SLC6A19, SLC7A1, SLC7A5, SLC1A1, SLC36A1, SLC7A11
Organismal injury and abnormalities: edema	ABCA5, ABI1, AHR, ATP2A2, BCR, C1S, CA1, CA12, CA2, CAV1, CBFB, CCND2, CD93, CLU, COL18A1, CTSA, CXADR, DOCK1, E2F3, ECE1, EDN1, EDNRA, ENG, ENPP2, ENTPD1, ERCC6, F2R, F2RL1, F3, FBXW7, FCGRT, FKBP1A, FLNA, FLRT2, FLT1, FOXP1, GATA6, **GJA1**, GPX2, HGF, HHEX, HIF1A, HMOX1, HSD17B7, IFT57, IGF2, IKBKB, IRAK3, ITGAV, JUN, PECAM1, PLAT, PODXL, POR, PRKAR1A, PTGER4, RXRA, SCP2, SERPING1, SETD2, SIRT1, SLC12A2, SMAD5, **SMAD7**, SOD3, SPRED1, SYK, TGFB1, TIMP3, TNFAIP6, UBE4B
Protein metabolism: degradation of protein, metabolism of protein	ANPEP, CASP6, CASP7, CAST, CAT, CAV1, CBLC, CD46, CDC37, CDKN2AIP, CTSB, CTSC, CTSD, CTSH, FBXL12, FBXL4, FBXO3, FBXO32, FBXO8, **GJA1**, **IL1RN**, IRAK3, ITCH, LAMP2, LNX1, LPL, MMP12, MMP2, **MMP3**, MYLIP, SERPINA1, SERPINB1, SERPINE2, TIMP3, TOPORS, VCP, **WNT5A**, EEF1A1, EEF2K, EIF2B2, EIF2B3, EIF2B4, EIF2B5, EIF2S1, EIF2S2, EIF3B, EIF3I, EIF4A1, EIF4B, EIF4E2, EIF4EBP2, EIF4G1, EIF5B, ETF1, **IL7R**, INSR, IRS1, ITGA2, JUN, LARP4B, LYN, MARS, SENP3, SERINC1, SERP1, SLC46A1, SLC7A1, SNRNP70, STIP1, THBS1, TNFRSF9, TNFSF10
Tissue Morphology:	APP, KLF4, PTEN, SLC4A2, TFF2, TGFA, BMP8B,

quantity of glandular epithelial cells	CXCL12, EPAS1, IL6ST, SMAD5, TGFB1, **WNT5A**, ZFX, ZNF148

Supplementary Table 2B. Main biological functions significantly perturbed in deregulated genes in active UC versus non-IBD controls (pattern 1 of gene expression, Figure 2).

Biological functions	**Genes**
Cell death: apoptosis of tumor cell lines, cell death of endothelial cells, necrosis, cell viability, cell death of blood cells, cell survival, apoptosis, cell viability of tumor cell lines, cell death of immune cells, cell death, cell death of connective tissue cells	**NFKBIZ**, KLF7, SPIB,NCOA7, MNDA, FOXQ1, EGR3, PARP14, PHTF1, ELL2, CEBPD, ETV7
Cellular growth and proliferation: proliferation of cells, proliferation of endothelial cells, colony formation of cells, proliferation of blood cells, proliferation of fibroblasts, proliferation of tumor cell lines, proliferation of connective tissue cells, proliferation of immune cells, colony formation of tumor cell lines	SOCS 3, SOCS1, IFI6, HSP90B1, IFI16, RIPK2, CASP1, PRLR, TIMP3, ELMO1, PROK2, BIRC3, BCL2A1, CD27, ITGB2, CKAP2, IL8RB, CYCS, DDIT4, TRIM69, AIFM3, IL17A, GZMB, GPR65, RASSF5, EAF2, TGM2, SEMA4D, CEBPB, IL1A, **IL1B**, CD38, DLC1, SRGN, AGT, BCL6, CASP4, COP1, **REG1A**, REG1B, VEGFC, S1P1, RETNLB, IFITM1, BCAT1, REG3A, TIMP2, PTGS2, SHH, CRIP2, BCL6, IHH
Cellular movement: migration of cells, homing, cell movement of PBMCs, migration of tumor cells, infiltration of blood cells, recruitment of antigen presenting cells, cell movement of fibroblast cell lines, chemotaxis, cell movement of antigen presenting cells, recruitment of cells, cell movement of endothelial cells	NCF2, NCF4, MMP9, RHOH, CYBB, CD27, IL17A, IL1A, **IL1B, IL8**, CCL2, CXCL2, PF4, IL17RB, CCR10, **CXCL5**, CCL24, CCR2, TNFRSF17, CXCL6, CSF2RB, CXCR4, IL8RB, OSMR, IL15RA, CSF3R, **IL7R**, VEGFC, GHR, PRLR, CXCL10, CCL3, CCL4, CSCL11, CXCL9, IFNAR2, PF4, OSRM

Hematological system development and functional communication: quantity of hematopoietic cells, development of lymphocytes, development of blood cells, development of leukocytes,	CCL3, CCND1, CCND3, CCR2, CCR7, CD19, CD2, CD74, CD79A, CD81, CD86, CD9, CDK13, CDK6, CDKN1B, CEBPA, CREB1, CREBBP, CRIP2, CSF1R, CSF2RB, CUX1, CXCL11, CXCL12, CXCR4, CYLD, DEF6, DFFB, IFNGR1, IFNGR2, IGF1R, IGF2, IGHM, IHH, IKBKB, IKZF1, IL12RB1, IL15RA, IL18, IL18R1, IL1A, **IL1B**, IL1R1, **IL1RN**, IL23A, IL27RA, IL2RA, IL2RB, **IL6R**, IL6ST, **IL7R**
Immune cell trafficking: infiltration by neutrophils, chemotaxis of leukocytes, adhesion of lymphocytes, adhesion of phagocytes, chemotaxis of phagocytes, chemotaxis of granulocytes, infiltration of granulocytes, infiltration of leukocytes, homing of phagocytes, chemotaxis of neutrophils, recruitment of antigen presenting cells, adhesion of immune cells, migration of neutrophils, chemotaxis of lymphocytes, cell movement of dendritic cells	NCF2, NCF4, MMP9, RHOH, CYBB, CD27, IL17A, IL1A, **IL1B, IL8**, CCL2, CXCL2, PF4, IL17RB, CCR10, **CXCL5**, CCL24, CCR2, TNFRSF17, CXCL6, CSF2RB, CXCR4, IL8RB, OSMR, IL15RA, CSF3R, **IL7R**, VEGFC, GHR, PRLR, CXCL10, CCL3, CCL4, CSCL11, CXCL9, IFNAR2, PF4, OSRM
Inflammatory response: response of phagocytes, response of macrophages, inflammatory response, immune response of phagocytes, activation of leukocytes, cell movement of neutrophils, activation of antigen presenting cells, immune response of antigen presenting cells, activation of phagocytes, immune response of cells, activation of mononuclear leukocytes, activation of lymphocytes	IFI30, CD74, HLA-DRA, HLA-DRB5, HLA-DRB1, HLA-DMA, TAP2, **DEFB4**, DEFA5, DEFA6, S100A12, NOS2A, CSF3R, NLRP7, SP140, MX2, CYSLTR1, DARC, RTP4, TLR8, IL17RB, TLR1, NLRP1, TOLLIP, IGHM, IGL@, IGKC, IGHG1, IGHG3, IGHD, CLEC4E, CD64, IGHA1, **LILRB1**, **LILRB2**, GBP1, GBP5, GBP2, PAG1, SAMHD1, FCGR2C, FCGR3B, SERPINB4, LCP2, MICB, CLEC7A, CD93, **VNN1**, **IL8**, CD27, GPR65, CEBPB, BST2, TREM1, IFITM2, IGFS6
Tissue morphology: quantity of lymphocytes, quantity of blood cells, quantity of leukocytes, quantity of antigen	**MMP10**, MMP28, MMP7, MMP9, PLAU, SERPINB4, SERPINE2, ADAM9, CAPN13, CPA3, MME, COLA42, MFAP2, ADAMTS5, FBN1, TIMP3,

presenting cells, invasion of cancer cells, apoptosis of tumor cells, progression of tumor	NTN2L, BGN, MMRN2, E-SELECTIN, SELPLG, **VCAN**, L-SELECTIN, P-SELECTIN, ITGAM, PECAM1, ICAM1, ITGB2, JAM2, CLDN8, CLDN2, CLDN23, CLDN1, CD86, VWF, COL4A2, CD44, ITGA8, CLEC4A, SLAMF7, CD300A, NRP1, PTPRC

Planell N et al. Supplementary Material

Supplementary Table 3. Comparison of relative changes in gene expression as assessed by microarray and real-time RT-PCR analysis. Microarray analysis was performed for 36 samples (cohort 1) and real-time RT-PCR for an independent group of 30 individuals (cohort2). Gene expression differences between groups are expressed as log2 ratio. Technical validation was performed by Pearson's correlation test on 15 samples from cohort 1 that had been analyzed by both methods. A p-value< 0.05 was considered statistically significant.

	Microarray (cohort 1)		Real-time RT-PCR (cohort 2)			
Gene Symbol	log2 ratio CUI/Ctrl	log2 ratio CUA+/Ctrl	log2 ratio CUI/Ctrl	log2 ratio CUA+ / Ctrl	Pearson correlation(r)	p-value
ABCB11	-2.049	-2.117	-0.061	-1.299	0.817	0.0002
ABCG2	-4.828	-5.766	-2.237	-3.055	0.985	$3.23x10^{-11}$
ACOX1	-2.137	-1.769	-0.957	-1.117	0.936	$3.04x10^{-07}$
ACSL4	1.508	1.802	1.237	2.602	0.894	$6.87x10^{-06}$
ADH6	-1.757	-1.353	-0.729	-1.191	0.927	$6.49x10^{-07}$
AQP3	2.697	2.265	2.015	1.624	0.949	$6.55x10^{-08}$
AQP8	-5.658	-8.614	-3.238	-5.901	0.964	$3.04x10^{-08}$
CCL18	1.254	3.930	0.548	2.754	0.980	$1.46x10^{-10}$
CCL20	0.295	2.054	0.874	0.484	0.991	$7.36x10^{-12}$
CD180	0.580	1.319	0.658	1.684	0.877	$1.80x10^{-05}$
CHI3L1	1.865	6.871	3.619	9.290	0.939	$2.19x10^{-07}$
COL1A2	1.101	2.521	0.155	2.805	0.974	$9.51x10^{-10}$
CXCL1	1.140	5.437	0.928	4.398	0.980	$1.79x10^{-10}$
CXCL3	1.125	4.436	0.932	3.526	0.989	$3.16x10^{-12}$
CXCL5	-0.137	6.092	2.004	5.529	0.974	$9.32x10^{-08}$
DEFB1	-3.198	-3.687	-0.945	-1.710	0.970	$2.43x10^{-09}$
DEFB4	0.287	5.919	---	---	-0.158	0.6622
GJA1	2.382	2.857	1.057	2.071	0.921	$1.08x10^{-06}$
IGHG3	0.004	2.874	0.432	5.894	0.828	0.0159
IL1B	0.411	4.524	1.402	4.226	0.988	$4.40x10^{-11}$
IL1RN	4.910	6.035	2.990	3.667	0.977	$2.19x10^{-09}$
IL6R	-0.967	-1.068	-0.512	-0.771	0.829	0.0001
IL7R	1.742	2.918	0.379	1.243	0.941	$5.36x10^{-07}$
IL8	-0.441	4.986	0.710	4.887	0.970	$1.05x10^{-08}$
IRF6	-0.873	-0.836	-0.366	-0.951	0.860	$3.92x10^{-05}$
LILRB1	1.257	1.929	---	---	0.343	0.2112
LILRB2	0.811	2.161	0.882	2.868	0.820	0.0002
ME1	2.301	2.795	2.727	2.509	0.977	$4.61x10^{-10}$
MEP1B	-3.487	-3.182	-1.161	-0.780	0.940	$2.00x10^{-07}$
MMP1	4.622	6.949	3.783	6.805	0.968	$3.55x10^{-09}$
MMP10	1.390	5.597	3.376	5.610	0.908	$2.84x10^{-06}$
MMP3	3.446	7.474	4.497	8.471	0.878	$1.69x10^{-05}$
MUC20	-0.936	-0.470	-0.074	-0.598	0.888	$9.80x10^{-06}$
MUC4	1.070	1.519	0.517	0.343	0.907	$3.15x10^{-06}$
MUC5B	1.723	1.790	0.798	0.950	0.864	0.0002
NFKBIZ	0.136	1.903	0.072	1.560	0.964	$8.03x10^{-09}$
OSTalpha	-4.591	-4.554	0.986	-0.283	0.942	$1.53x10^{-07}$
PRAP1	-4.201	-4.102	-1.672	-1.073	0.986	$1.54x10^{-11}$
REG1A	0.498	10.822	1.757	10.413	0.922	$7.42x10^{-06}$
REG4	3.845	5.021	4.504	4.651	0.995	$2.78x10^{-14}$

RUNDC3B	-1.871	-2.782	-1.187	-1.618	0.963	$9.42x10^{-09}$
S100P	2.902	2.684	3.698	3.102	0.971	$1.78x10^{-09}$
SERPINB5	4.613	5.794	3.927	3.318	0.995	$1.64x10^{-14}$
SLC16A1	-2.939	-2.833	-1.526	-1.802	0.971	$1.66x10^{-09}$
SMAD7	-1.039	-1.141	-0.586	-0.938	0.816	0.0002
TFF1	1.788	1.926	2.576	3.284	0.941	$1.68x10^{-07}$
TFPI2	2.460	2.592	2.664	3.729	0.769	0.0021
TGFBI	1.650	2.627	1.032	2.566	0.945	$1.15x10^{-07}$
TIMP1	2.585	4.195	1.987	3.450	0.978	$2.83x10^{-10}$
TJP1	-0.981	-0.686	-0.430	-0.128	0.691	0.0044
TRIM29	3.419	4.018	3.300	2.976	0.892	$7.74x10^{-06}$
VCAN	1.191	1.999	0.183	1.953	0.928	$6.23x10^{-07}$
VNN1	0.456	4.712	0.762	0.588	0.971	$2.02x10^{-09}$
WNT5A	1.229	2.740	-0.166	2.357	0.964	$6.93x10^{-09}$